Indian Journal of Biochemistry & Biophysics
Vol. 60, December 2023, pp. 941-957
DOI: 10.56042/ijbb.v60i12.6278

Computational approach on *Moringa oleifera* as an inhibitor against SARS-CoV-2 structural proteins

Preethi Ramakrishnan[1#], Pandiselvi Pandi[1], Muralidharan Jothimani[2#], Sakthi Sasikala Sundaravel[2], Karthikeyan Muthusamy[2], Unnamalai Narayanan[1], Mehboobali Pannipara[3], Abdullah G Al-Sehemi[4] & Arunkumar Jayaraman[1]*

[1]Shri AMM Murugappa Chettiar Research Centre (MCRC), Taramani, Chennai- 600 113, Tamil Nadu, India

[2]Pharmacogenomics and CADD Lab, Department of Bioinformatics, Alagappa University, Karaikudi- 630 003, Tamil Nadu, India

[3]Research Centre for Advanced Materials Science; & [4]Department of Chemistry, King Khalid University, Abha-61413, Saudi Arabia

Received 18 October 2023; *revised 13 November 2023*

The lethal pandemic has been brought on by the emergence of the SARS-CoV-2. The moringa leaves have a rich nutritional value in the host immunity and act as an immune booster against SARS-CoV-2. Tea was formulated from the moringa leaves, and dried at ambient temperature for serving health benefits. The results provide evidence that the application of heat on moringa leaves improves the flavor and quality of tea without degrading the nature of phenolic and flavonoid compounds present in moringa leaves. The molecular docking result among the screened compounds from moringa leaves has a good docking score varying from -10.657 to -13.735 kcal/mol for the Main protein, while Spike glycoprotein has a docking score ranging from -8.559 to -10.522 kcal/mol and Membrane protein docking score from -7.208 to -10.411 kcal/mol. The atomic configuration and electron profile of the docked complex were subjected to the DFT calculations. The molecular dynamics simulation study shows that the selected compounds have maintained stable conformation in the simulation period and interact with the target. Thus, we conclude that *Moringa oleifera* leaves compounds to support the antagonist activity against SARS-CoV-2's structural proteins and the leaf-based product could be a good immune booster for SARS-CoV-2 infection.

Keywords: Coronavirus, Immune booster, Molecular docking, Moringa Tea, Phytochemicals

Moringa oleifera Lam. a miracle tree is cultivated in subtropical and tropical regions, potential for its nutritional and medicinal properties. The bark, leaves, seeds and roots of moringa are rich in minerals, carbohydrate, protein, fats, fiber, and also contain significant amounts of iron, calcium, vitamins such as A, B and C, hence all the part of the plant is used for food, medication and industrial purposes[1,2]. The moringa leaves also attributes with several Phytochemicals such as carotenoids, flavonoids, saponins, steroids, tannins, terpenoids, alkaloids, anthocyanin, anthraquinone, cardiac glycosides etc., which are potent to possess antioxidants, antimicrobial, antifungal, antiviral activity antihypertensive, antitumor, anticancer, antihyperlipidemic, antipyretic, and anti-inflammatory properties[3,4]. The nutrients and phytochemicals present in the leaves play an important role in activating enzymes and hormones that enhance the growth, function, and maintenance of life process in both human and animals[1,5].

The moringa leaves act as a valuable food for the malnutrition children, pregnant and lactating women. The leaves are generally consumed in the form of vegetable curry, soup or seasoning by both rural and urban population, due to the health awareness about moringa, alongside value added products (noodles, bread, Chutney, biscuits, cakes and porridge)[6-9]. The leaves can be consumed as fresh or after boiling or it can be dried and used in the form of powder for culinary purpose[10]. Due to the presence of phenol and flavonoids in the leaves, the research is focused on development of moringa leaves extract as beverage like tea or soup. The Phytochemicals in tea act as free radical scavenger and induce the human immunity that manages the blood pressure, glucose level and serve as an energy booster[11]. Hence, tea was formulated as a value-added product of moringa leaves, which can be prepared and consumed by people of all economic classes, particularly those in rural areas of India. This tea will energize their life better with the locally available moringa leaves. The

*Correspondence:
[#]Authors were equally contributed for the first Authorship
Phone: 0091-44-22430937
Fax: 0091-44-22430369
E-mail: arunkumarj@mcrc.murugappa.org

moringa tea or soup, which was developed in our laboratory, was cultivated under organic cultivation system.

Most of the plant-based food has antinutrient properties, which possess the property to reduce the bioavailability of nutrients in our body. Antinutrient factors like cyanide, oxalate, phytate and inhibitors are present in the leaves of moringa, to overcome the negativity of this antinutrient property, the leaves should be processed without losing the nutritional and phytochemicals property[12]. To retain the Phytochemicals, present in the leaves, to reduce the raw flavor and to increase the color of the tea, the leaves were processed under various conditions. Covid-19 infections often lead with multi-pathogenic consequences and have an impact on human vital organ functions. With everything looked at severe acute respiratory syndrome corona virus 2 (SARS-CoV-2) Pandemic, potent inhibitors were in need to rejuvenate the molecular mechanism of human condition. *Moringa oleifera* leaves were employed in this study accordance with the literature survey for a search of natural inhibitor. Rather, studies also suggest that moringa leaves play a vital role for the host immunity and their active compounds act as a supplemental food source and an immune booster for the life threatening SARS-CoV-2. Through the *in silico* approaches a huge number of moringa leaves compounds were screened for antiviral activity versus the SARS-CoV-2 in a short period of time. This study's main objective was to figure out the potent compounds of moringa leaves for inhibiting SARS-CoV-2 structural proteins. For this approach, we employed molecular docking, molecular Dynamics, Density Function Theory (DFT) and ADME/T analysis for protein-ligand complex by using the Schrodinger 2018-4 suite[13-15].

Materials and Methods

Materials and sample preparation

Moringa leaves (*Moringa oleifera*) of the PKM 1 variety were collected from the farm of the Shri AMM Murugappa Chettiar Research Centre in Chennai, Tamil Nadu, India. The leaves were thoroughly washed to remove any dirt and then dried at room temperature to retain the phenols and flavonoids.

Determination of total phenol

The presence of phenol in tea was determined by the Folin-Ciocalteu method. About 1 mL of tea extract was mixed with 2.5 mL of Folin-Ciocalteu reagent (1:10 *v/v* in distilled water) and allowed it for 5 min; later 2 mL of 4% sodium carbonate was added. The mixture was shaken well and incubated for 2 h under dark condition. After incubation, the samples were measured at 740 nm using UV-visible spectrophotometer (Biospectrometer, Make: Eppendorf) and the total phenol was calculated based on the standard graph generated using gallic acid ranging from 20 µg to 100 µg[16].

Determination of flavonoid

The presence of the flavonoid in tea was determined using aluminum chloride. Sample of about 1 mL of mixed with 3 mL of 5% aluminum chloride and incubated for 30 min. After the incubation period, 3 mL of distilled water was added and the absorbance value was measured at 437 nm. The amount of the flavonoid present in tea was calculated using the standard quercetin with the concentrations ranging from 200 µg to 1000 µg[17].

Determination of free radical scavenging activity

The 2, 2-diphenyl-1-picrylhydrazyl (DPPH) method was used to determine the free radical scavenging activity of the prepared tea or soup. About 100 µL of tea was added to 500 µL of DPPH solution and incubated it under dark for 20 min. The concentration of DPPH in the reaction mixture was measured at the wavelength of 515 nm[18]. The radical scavenging activity was measured using the below mentioned formula:

$$Free\ radical\ scavenging\ activity\ (\%) = \frac{Abs\ of\ Control - Abs\ of\ Sample}{Abs\ of\ Control} \times 100$$

Reducing power assay

The antioxidant activity of the tea extract was measured by using reducing power assay. The extract (1 mL) was mixed with 5 mL of 0.2 M phosphate buffer (pH 6.6) and 5 mL of 1% potassium ferricyanide, immediately the mixture was mixed well and incubated at 50°C for 20 min. After incubation, to stop the reaction, 5 mL of 10% trichloroacetic acid was added to the mixture and centrifuged at 3000rpm for 10 min. Then 5 mL of supernatant was taken out separately and it was diluted with 5 mL of distilled water and 1 mL of 0.1% ferric chloride was added in the test solution and measured at the wavelength of 700 nm using UV-visible spectrophotometer[19]. The obtained absorbance value was directly proportional to the reducing power. All the assays were carried out in triplicate and the

results were expressed as mean values ± standard deviation.

Sensory evaluation

Twenty semi trained panelists were involved in the analysis. All the samples were arranged in a random sequence label with different code. A nine-point hedonic scale was used for the evaluation.

Target protein structure preparation

The X-ray crystal structure of SARS-CoV-2 structural proteins Main Protein (PDB Accession ID: 6LU7), Surfaces Spike-Protein with ACE-2 (PDB Accession ID: 7BZ5) was retrieved from RCSB PDB. Furthermore, the left over member of SARS-CoV-2 structural proteins, due to lack in PDB structure Membrane Protein was modeled through the protein structure prediction tools of the I-Tasser server[20]. The modeled membrane protein was generated and top hit model was chosen based on C-score. Thus, protein structures were enhanced for preparation followed by the virtual screening and docking procedures.

Protein and ligand preparation

The three-dimensional structural proteins of SARS-CoV-2 were incorporated within preparation wizard of Schrodinger 2018-4 suite (MAESTRO) for protein preparation. These structures contain residues with the missing atom, side chains and varied bond orders. The preprocess takes place for adding the missing atoms in the protein structure as well as the exclusion of water molecules. The structural optimization along with minimization was done using the force field (OPLS-2005) to fix backbone atoms. Further, the site map is generated for the protein structures to locate its specific binding site. Top scored sites were predicted and for the chosen site receptor grid was generated. Thus, output grid file was generated to perform virtual screening (VS) in order to categorize the potent compounds.

For the ligand preparation in the Schrodinger 2018-4 suite, the LigPrep module was employed. To prepare the moringa leaf compounds for virtual screening, the whole set of compounds are retrieved from PubChem database. The conformers were generated for each and every compound minimization step using OPLS3 force field. The conformers with high energy were filtered and removed with a parameter set for 1Å of minimum atom deviation range. For the generated conformers the ligand preparation was done and processed for virtual screening[21,22].

Virtual screening

The virtual screening (VS) module was employed to identify the potential antagonic compound from moringa leaves for targeting SARS-CoV-2 structural protein using Schrodinger suite 2018-4 (MAESTRO) for targeting the and the compound prepared from the. This structure based workflow is calculated by using the OPLS3 force field and further the molecular docking approach for compound screening takes place using Glide docking. The screened top hits for SARS-CoV-2 structural protein were listed based on the score/parameters of molecular docking protocol[23-25].

Density-functional theory (DFT)

The calculation for DFT was performed in jaguar module of Schrodinger on the top hit compounds using the virtual screening procedure. The complete geometrical refinement for the selected top hits were calculated based on the HOMO, LUMO and MESP parameters. These DFT computation parameters were obtained based on the basic sets of 6-31G∗ followed by three parameters of Becke's hybrid functions along with Lee-Yang-Parr's (LYP) correlation functions (B3LYP). The transition of electron state reveals that the energy gap obtained was calculated to analyze the ligand stability and reactive state by using HUMO, LUMO and MESP parameters[26,27].

Molecular dynamics (MD) simulation

Molecular Dynamics (MD) simulations were performed to confirm the backbone flexibility stability of SARS-CoV-2's structural proteins using GROMACS version 2022.3 (Groningen Machine for Chemical Simulations) package. The analysis on the flexibility of the SARS-CoV-2's protein provides details on the structural properties of the modeled and complex protein. The calculations indicate that all atoms that were immersed in the water molecules were also present in the corresponding particles. The volume, temperature, pressure, potential energy and total energy enhances the spatial properties for stabilizing targeted protein of interest. The topology generation for protein is accessed by Gromacs software utilities and for ligand topology ATB server is used[28,29]. SPC water molecules model were solvated to eliminate irrelevant atomic contacts under periodical defined conditions. To maintain the appropriate net neutral charge, ions (Na^+ or Cl^-) were countered throughout the system for maintenance. The energy minimization were done using the force field (GROMOS96 54a7)[30]. The Van

der Waals force was set to 9Å along with Ewald's simulation technique to calculate the electrostatic interactions for long progress. The algorithm of Berendsen thermostat was applied for maintaining the constant temperature at 300 K of coupling interval 0.1ps for NVT followed by pressure maintenance of 1bar for NPT. The constraint solvers (SHAKE) and (LINCS) algorithms were applied for the bond length and geometrical constraints of protein present within water molecules respectively. Finally, the complexes were produced with MD simulations that lasted 50 nanoseconds (ns) and apo structure dynamics with 100 ns. The RMSD, RMSF hydrogen bond and calculations were used to determine the protein's structural alterations and dynamic behavior. The outputs were generated and the graphs were plotted[31,32].

ADME/T Prediction

The compounds ADME calculation was performed using QikProp of Schrodinger's 2018-4 module and toxicity profile was calculated using the server PROTOX https://tox-new.charite.de/protox_II. QikProp is a user friendly and accurate suite in predicting the physical descriptors and therapeutically important characteristics of organic compounds, individually or in batches. The compounds retrieved from the repository databases should obtain 3D-structure not a 2D one and explicit mention of hydrogen atoms. A thorough investigation was done with Qikprop to quickly forecast the principal descriptors with ADME/T characteristics of each compounds. Qikprop provides parameters for evaluating a specific molecule's characteristics in comparison to 95% of recognized drugs. The investigation parameters like Lipinski's rule of five, Cell line permeability (QPPCaco), Madin-Darby Canine Kidney cell permeability (QPPMDCK), Predicted Octanol/water partition Co-efficient (QPlogpo/w) and Human Oral Absorption (HOA%) were evaluated to find the potent hit from obtained compounds and further provided for the drug discovery process. Toxicology predictions were made using the ProTox-II server. Every compound was examined separately using organ toxicity and toxicity end points criteria. A scale from 1 to 6 was used to estimate the lethal dosage (LD50) value (acute oral toxicity in rats) and toxicity classes. Each defined category is presumptive with regard to the pharmacokinetic properties of the selected lead drugs[33-36].

Results and Discussion

As a preliminary experiment, moringa leaves dried under room temperature was used for the moringa tea preparation using the boiling method. The prepared moringa tea was subjected to sensory evaluation with 20 members. Various characteristics such as tea appearance, color, flavor, taste and overall acceptability were determined by the evaluators. The results of the moringa tea evaluated by the panel are given in the table with standard error (Table 1).

The major comment received from the panel members was that the tea contains raw moringa flavor with bitter taste. The flavor and taste were little better; hence a trial study was carried out on processing the moringa leaves under various conditions to overcome the stated comments about flavor and bitter taste. The presence of phenolic compounds like tannins, which are astringent and bitter, might have caused dry and pucker feeling in the mouth[37].

The polyphenols and flavonoids were the major cause for the expression of astringent bitter taste of tea[38]. The processing of the leaves may alter the nature of the compounds responsible for astringent and bitterness taste. Till now, there is no research work on identifying the individual or group of compounds in maintaining the standard quality of moringa tea. Various compounds present in moringa possess various health benefits, despite astringent and bitter tastes, which are unpleasant. They are desirable at moderate amounts considering the health benefits of flavonoids and phenols present in tea. Therefore, the moringa leaves were subjected to various treatment processes to reduce the strong flavor, astringent / bitter taste and to improve the color of the tea.

Moisture content

The moisture content of all the moringa leaves, which were processed under different conditions falls within the range of 9-11%. The moringa leaves, blanched for three min showed the maximum moisture (11%) content when compared with other processed leaves under various conditions. No significant variations in results were observed among the various treatments except blanching.

Table 1 — Sensory evaluation of moringa tea

Parameters	Percentage (%)
Appearance	79±0.7
Color	76±0.7
Flavor	67±1.3
Taste	65±1.7
Overall acceptability	72±1.4

Scan analysis of moringa tea

The color of the tea is an important factor, which should be appealing to attract people to taste it. The color of the tea was evaluated through visual observation. The color of the tea was increased as the exposure period increased and the color was reduced after 3 min exposure in the microwave, blanching and steaming, and in hot air oven exposure over 3 h the color was reduced (Figs 1 & 2). The reason for the color reduction may be due to the degradation of few phytochemical compounds, which were sensitive to overheating. The color of the tea prepared from the leaves processed at hot air oven for 2 h found to be reddish brown in color and the raw moringa flavor was reduced significantly. Meanwhile, the bitter taste also reduced, which was acceptable in both tea bag and boiling method.

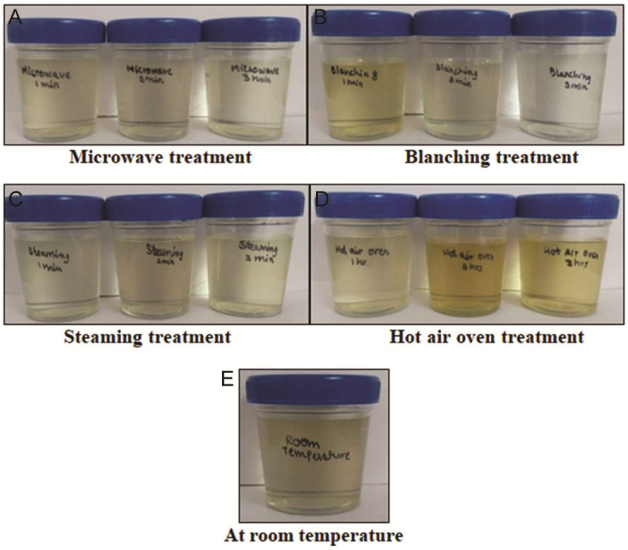

Fig. 1 — Color of tea prepared through boiling using tea bag

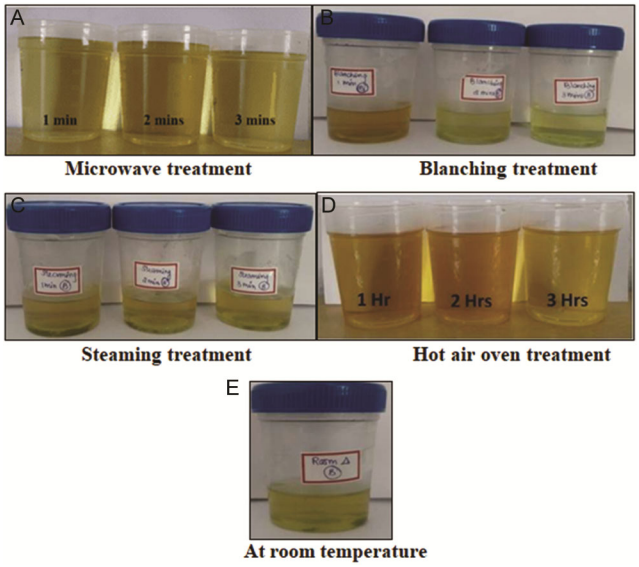

Fig. 2 — Color of tea prepared through direct boiling

To detect the presence of phytochemicals in the moringa tea, samples were analyzed by scanning the extract in UV-Visible spectrometer from 200-800 nm. Two peaks were observed in all the processed moringa leaf tea, first peak was in the wavelength range from 258-260 nm and the second peak found in the wavelength range from 323-326 nm. Both these peaks were observed in tea prepared using tea bag and direct boiling. The scan analysis results corroborated with the results of the color, the absorption value was decreased as exposure increased in microwave, blanching and hot air oven treatments group except steaming treatment. When compared with the other treatments based on color and absorption values the hot air oven exposure showed better color and high absorption value. The absorption value increased due to the activation of polyphenols and flavonols present in the tea, when the leaves exposed to heat. Further, the presence of phenols and flavonoids, and their impact on their activity was determined by various assays.

The color of the tea prepared from the leaves processed in hot air oven for 2 h was found to be reddish brown in color and the raw moringa flavor also subsided. Meanwhile, the taste of bitterness also reduced, which was acceptable in both tea bag and boiling method.

Total phenol and flavonoid contents of the tea

The effect of various treatments on the phenolic and the flavonoids content of moringa tea prepared using tea bag and direct boiling method. The results revealed that phenols present in the moringa leaves gradually decreased as the exposure period increases in all the three treatments such as blanching (381-216 µg/ mL), steaming (421-322 µg/ mL) and hot air oven (352-304 µg/ mL) except the microwave treatment (419-435 µg/ mL), the leaves treated at room temperature showed 389 µg/ mL. Whereas, in microwave exposure the phenolic content was increased as the exposure time increased due the release of bound phenol compound in the cells membrane. The phenolic content was found to be more in the tea prepared using direct boiling method, where maximum phenolic compounds were released than the tea prepared using a tea bag (19-55 µg/ mL). Similarly, the flavonoid compounds were also increased in microwave (554-625 µg/ mL), steaming

(457-516 µg/ mL) and hot air oven (352-304 µg/ mL) expects blanching method (365-512 µg/ mL), which indicates the release of flavonoid compound when exposure period increases under temperature or irradiation. The release of flavonoid was observed to be less in tea bag method for the treatment group, the values fall within the range of 161-512 µg/ mL. The availability of phenolic or flavonoid compounds in moringa leaves depends on various factors like the conditions of soil and its nutrient factor, climatic zone, and suitable temperature in which the compound extracted under various conditions[39].

Researchers also found that gamma irradiation influences the phenolic and flavonoid content in the moringa and increase the antioxidant[40], which adds the credits to our results that temperature or irradiation increase or decrease the phenolic or flavonoid content in the moringa tea. On the other hand, research conducted at *M. stenopetala* leaf showed the highest amounts of total flavonoid using decoction for 5 min extract due to the longer exposure of leaves to heat, whereas the lowest amounts of flavonoid were obtained in cold water extraction[41].

Antioxidant and reducing power of moringa tea

The presence of antioxidants and their free radical scavenging activity were measured by DPPH and ferric reducing antioxidant power assays. The scavenging effects were found to be more for the treated moringa leaves at microwave (85-90 %) and hot air oven (87-85 %). The antioxidant activity was observed in all the tea prepared from the processed leaves at different conditions than the leaves dried under room temperature (48 %), which indicates that the content of phenol or flavonoid increasing under exposure to various conditions, so it proportionally increases the antioxidant activity. Similarly, the reducing power was also found to be more in the processed leaf tea (91 – 149 % inhibition) than the room temperature (48 %), especially microwave treatment (113-149 % inhibition) possess more reducing power. Overall, the activity was less for tea prepared through tea bag method as compared with direct boiling method. Research work of Pham *et al*[42] showed that, *H. hirsute* L. leaves processed under hot-air drying at 80°C showed the significant levels of polyphenols, flavonoids and saponins than leaves treated under low temperature and infrared drying. Similarly, earlier report on antioxidant and total phenolic content, which was increased in *Smallanthus sonchifolius* peels when it was heated at 100°C for 60 min[43]. Another study evaluated the changes in phenolics, which varied significantly with the heating time and temperature increased till 130°C[44]. All these research findings supported the present research work and proved that moringa leaves treated at hot air oven for two h possess more flavonoid and phenols, which were found to exhibit strong antioxidant with high reducing power.

Apo –dynamics Simulation

The MD simulation run were performed thoroughly in the solvated water molecule to evaluate the stability and conformational changes of the modeled SARS-CoV-2's protein**.** This study outcome demonstrated that the model is relatively stable in the natural state and the MD simulation meets the demand for energy efficiency. The model is generated stably from 10000ps to 100000ps with a mean of 0.4 to 0.5Å of the deviation value, as evidenced by the backbone atoms RMSD (Fig. 3). Initially with the same range of runs from 1ps to 1000 ps of simulation, the simulation of any kind of complexes first attains the peak rise up value and attains the stability check. The RMSD production of MD investigations for SARS-CoV-2'sprotein have developed into a stable state. This shows that after 1000ps of simulation, the degree of compaction in the structure remains steady. The resulting model passed all the quality assurance tests, and it is thus suggested that this model has a good estimation of SARS-CoV-2's structure and may be used to describe different receptor-ligand complex interaction studies and to examine the link between the structure and function.

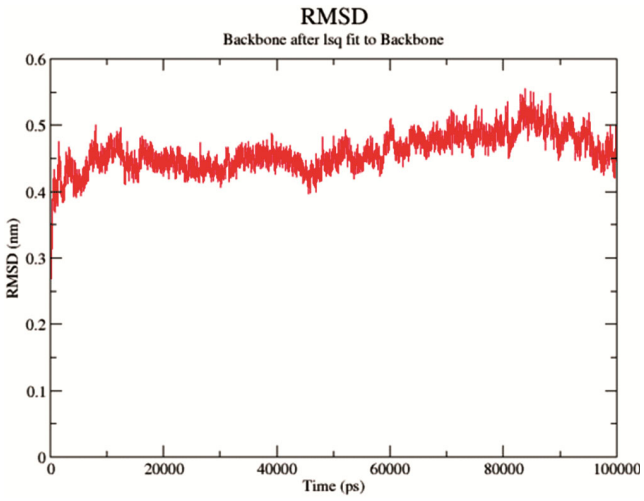

Fig. 3 — Backbone stability for the SARS-CoV-2 membrane protein

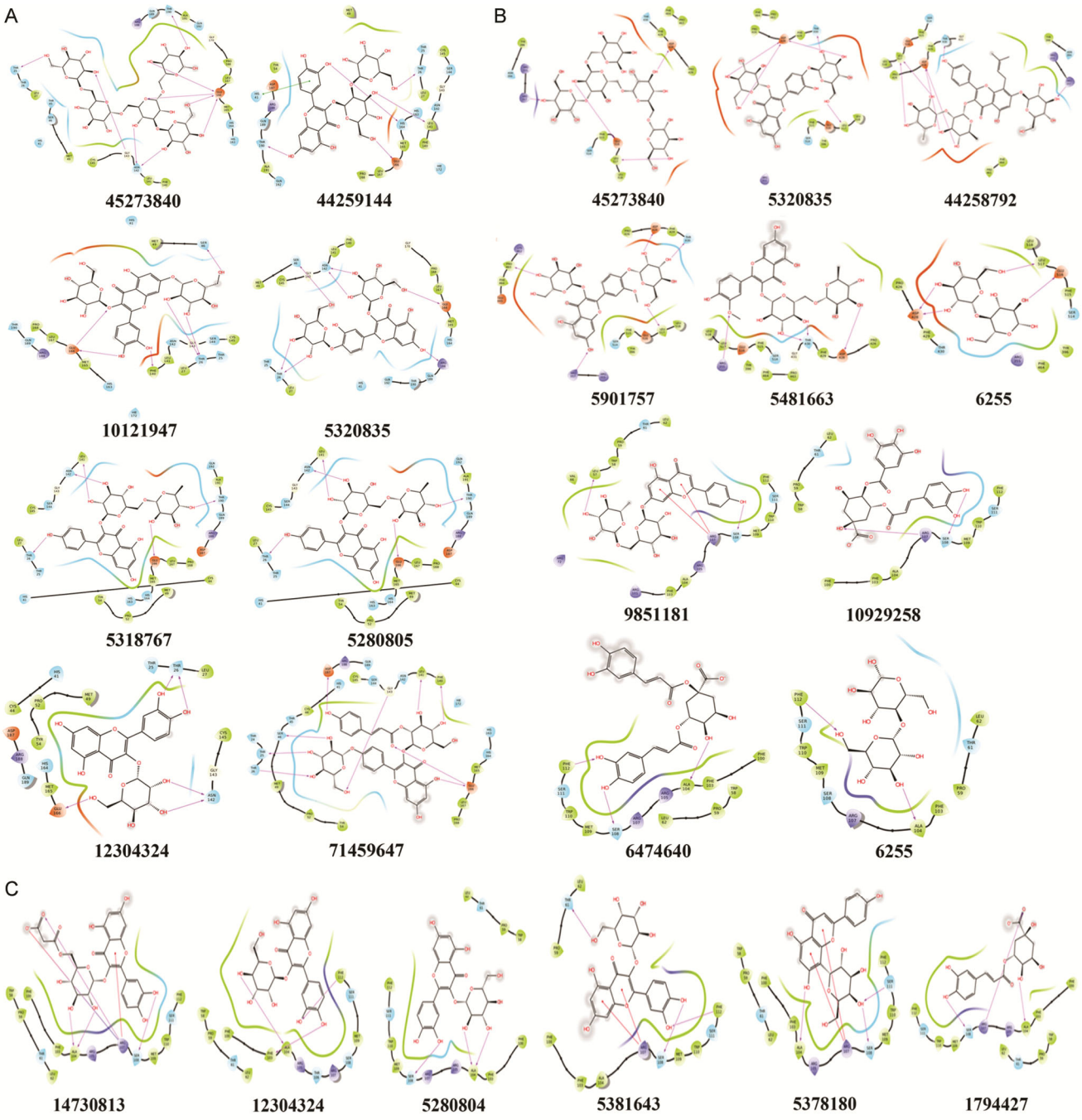

Fig. 4 — 2D-Interactions binding mode of *Moringa oleifera* leaves compound with SARS-CoV-2 (A) Main protein; (B) Spike protein; and (C) Membrane protein

Virtual screening against SARS-CoV-2's main protein with the *Moringa oleifera* leaves compound

A huge set of compounds from *Moringa oleifera* leaves compounds were docked against Main protein (PDB Accession id: 6LU7) of SARS-CoV-2 (Fig. 4A). The top hits 45273840, 44259144, 10121947, 5320835, 5318767, 5280805, 12304324 and 71459647 were chosen for their best scoring function against SARS-CoV-2 main protein (Table 2). Among them compound 45273840 strongly docked with a score -13.735 kcal/mol and their following amino acid residues ASN142, GLU166, GLY143, THR25, and THR190 are interacting with their compound. The compound 44259144 firmly docked with a score of -13.166 kcal/mol and interactive with the residues LEU141, GLU166, HIS41, HIS164, THR26, and

Table 2 — Virtual screening analysis of SARS-CoV-2 for its main protein with the *Moringa oleifera* leaves compound

Compound Code	Compound Name	Docking Score (kcal/mol)	Glide score (kcal/mol)	Glide Energy (kcal/mol)	Interacting Residues
45273840	D-Glucopyranosyl) -(alpha-1,6) -(D-glucopyranosyl)-(alpha-1,6)-(3-O-[D-glucopyranosyl)-(alpha-1,3)]-D-glucopyranosyl)-(alpha-1,6)-alpha/beta-D-glucopyranoside	-13.735	-13.735	-65.408	ASN142, GLU166, GLY143, THR25, THR190
44259144	Quercetin 3-sophoroside	-13.166	-13.195	-69.485	GLU166, HIS41, HIS164, LEU141, THR26, THR190
10121947	Quercetin 3,7-Diglucoside	-11.807	-11.807	-65.586	GLU166, PHE140, SER46, THR26
5320835	Quercetin 3,4'-diglucoside	-11.224	-11.225	-66.727	ASN142, ARG188, GLU166, SER46, THR26
5318767	Nicotiflorin	-11.117	-11.117	-71.482	ASN142, GLU166, LEU141, THR26, THR190
5280805	RUTIN	-11.045	-11.073	-68.205	ASN142, GLU166, HIS41, HIS164
12304324	Quercetin-3-O-d-glucopyranoside	-10.745	-10.773	-59.055	ASN142, GLU166, THR26
71459647	Allivictoside A	-10.659	-10.657	-64.752	ASP187, GLU166, GLY143, LEU141, PHE140, SER46, THR25, THR26

THR190 residues. The 10121947 compound attains the docking value of -11.807 kcal/mol and interactive with GLU166, PHE140, SER46, and THR26 residues. The compound 5320835 docked with a score of -11.224 kcal/mol and compound interactive with the residues ASN142, ARG188, GLU166, SER46, and THR26. The compound 5318767 obtains -11.117 kcal/mol as docking score and interacts with ASN142, GLU166, LEU141, THR26, and THR190 residues. The 5280805 compounds got a docked score with the value -11.045 kcal/mol interactive with their residues ASN142, GLU166, HIS41, and HIS164.The 12304324 compound obtained a docked score -10.745 kcal/mol with respective to the interaction of compound with ASN142, GLU166, and THR26 residues. The 71459647 compound attains the docked score of -10.659 kcal/mol, and interactive with their residues ASP187, GLU166, GLY143, LEU141, PHE140, SER46, THR25, THR26. Overall, residues interactions play a major role in SARS-CoV-2's main protein agonist activity.

Virtual screening against SARS-CoV-2's spike protein with the *Moringa oleifera* leaves compound

A huge set of compounds from *Moringa oleifera* leaves compounds were docked against spike protein (PDB Accession id: 7BZ5) of SARS-CoV-2 (Fig. 4B). The top hits 45273840, 5320835, 44258792, 5901757, 5481663, 6255, 13915496, 14730813, 107876 and 10088114 were chosen for their best scoring function against SARS-CoV-2 main protein (Table 3). Among them compound 45273840 strongly docked with a score -10.522 kcal/mol and their following amino acid residues ASP428, ARG357, GLU516, and LEU517 are interacting with their compound. The compound 5320835 firmly docked with a score -10.038 kcal/mol and interactive with the residues ASP428, LEU517, and THR430 residues. The 44258792 compound attains the docking value of -9.063 kcal/mol and interactive with ASP428, ARG357, LEU517, and THR430 residues. The compound 5901757 docked with a score of -8.996 kcal/mol and compound interactive with the residues ASP428, ARG357, LEU517, PRO463, and THR430. The compound 5481663 obtains -8.882 kcal/mol docked score and interacts with ASP428, ARG355, and THR430 residues. The 6255 compounds got a docked score with the value -8.846 kcal/mol and interactive with their residues ASP428, GLU516, and LEU517.The 13915496 compound obtained a docked score -8.654 kcal/mol with respective to the interaction of compound with ASP428, ARG355, LEU517, PHE464, and THR430 residues. The 14730813 compound attains the docked score of -8.625 kcal/mol, and interactive with their residues ARG355, ARG357, GLU516, PRO463, and THR430. The 107876 compound attains the docking value of -8.606 kcal/mol and interactive with ASP428, ARG355, and GLU516 residues. The compound 10088114 obtains -8.559kcal/mol as docking score and interacts with ASP428, ARG355, PHE515, and THR430 residues. Overall, residues

Table 3 — Virtual screening analysis of SARS-CoV-2 for its Spike protein with the *Moringa oleifera* leaves compounds

Compound Code	Compound Name	Docking Score (kcal/mol)	Glide score (kcal/mol)	Glide Energy (kcal/mol)	Interacting Residues (kcal/mol)
45273840	D-Glucopyranosyl) -(alpha-1,6)-(D-glucopyranosyl)-(alpha-1,6)-(3-O-[D-glucopyranosyl)-(alpha-1,3)]-D-glucopyranosyl)-(alpha-1,6)-alpha/beta-D-glucopyranoside	-10.522	-10.522	-45.706	ASP428, ARG357, GLU516 LEU517
5320835	Quercetin 3,4'-diglucoside	-10.038	-10.059	-48.969	ASP428, LEU517, THR430
44258792	Diphylloside B	-9.063	-9.063	-54.378	ASP428, ARG357, LEU517, THR430
5901757	Dactylin	-8.996	-8.996	-53.353	ASP428, ARG357, LEU517, PRO463, THR430
5481663	Narcissoside	-8.882	-8.911	-48.999	ASP428, ARG355, THR430
6255	Maltose	-8.846	-8.846	-37.190	ASP428, GLU516, LEU517
13915496	Kaempferol 3-neohesperidoside	-8.654	-8.683	-52.023	ASP428, ARG355, LEU517, PHE464, THR430
14730813	Quercetin 3-(6"-malonyl-glucoside)	-8.625	-8.653	-46.215	ARG355, ARG357, GLU516, PRO463, THR430
107876	Procyanidin	-8.606	-8.606	-52.864	ASP428, ARG355, GLU516
10088114	Gallic acid 4-O-glucoside	-8.559	-8.565	-32.324	ASP428, ARG355, PHE515, THR430

Table 4 — Virtual screening analysis of SARS-CoV-2 for its Membrane protein with the *Moringa oleifera* leaves compounds

Compound Code	Compound Name	Docking Score (kcal/mol)	Glide score (kcal/mol)	Glide Energy (kcal/mol)	Interacting Residues
14730813	Quercetin 3-(6"-malonyl-glucoside)	-10.411	-10.410	-42.135	ARG107, ALA104, SER108
12304324	Quercetin-3-O-d-glucopyranoside	-7.940	-7.969	-40.560	ALA104, PHE103, PHE112
5280804	Isoquercitrin	-7.766	-7.795	-35.980	ALA104, SER108
5281643	Hyperoside	-7.751	-7.780	-44.436	ARG107, PHE112, SER108, THR61
5378180	Flavone	-7.707	-7.742	-36.976	ALA104, ARG107, SER108, SER111
1794427	Chlorogenic acid	-7.564	-7.567	-33.081	ALA104, ARG107, SER108
9851181	Isorhoifolin	-7.532	-7.532	-55.231	ARG107, LEU57, SER108
10929258	4-O-galloylchlorogenic acid	-7.285	-7.285	-39.905	ARG107, SER108
6474640	1,3-Dicaffeoylquinic acid	-7.275	-7.275	-43.202	ALA104, PHE112, SER108
6255	Maltose	-7.208	-7.208	-29.964	ALA104, PHE112

interactions play a major role in SARS-CoV-2's spike protein agonist activity.

Virtual screening against SARS-CoV-2's membrane protein with the *Moringa oleifera* leaves compound

A huge set of compounds from *Moringa oleifera* leaves compounds were docked against spike protein (PDB Accession id: 7BZ5) of SARS-CoV-2 (Fig. 4C). The top hits 14730813, 12304324, 5280804, 5281643, 5378180, 1794427, 9851181, 10929258, 6474640 and 6255 were chosen for their best scoring function against SARS-CoV-2 main protein (Table 4). Among them compound 14730813 strongly docked with a score -10.411 kcal/mol and their following amino acid residues ARG107, ALA104, and SER108 are interacting with their compound. The compound 12304324 firmly docked with a score of -7.940 kcal/mol, and interactive with the residues ALA104, PHE103, and PHE112 residues. The 5280804 compound attains the docking value of -7.766 kcal/mol and interactive with ALA104 and SER108

residues. The compound 5281643 docked with a score of -7.751 kcal/mol and compound interactive with the residues ARG107, PHE112, SER108, and THR61. The compound 5378180 obtains -7.707 kcal/mol docked score and interacts with ALA104, ARG107, SER108, and SER111residues. The 1794427 compounds got a docked score with the value -7.564 kcal/mol and interactive with their residues ALA104, ARG107, and SER108.The 9851181 compound obtained a docked score -7.532 kcal/mol with respective to the interaction of compound with ARG107, LEU57, and SER108 residues. The 10929258 compound attains the docked score of -7.285 kcal/mol, and interactive with their residues ARG107, and SER108. The 6474640 compound attains the docking value of -7.275 kcal/mol and interactive with ALA104, PHE112, and SER108 residues. The compound 6255 obtains -7.208 kcal/mol, docking score and interacts with ALA104 and PHE112 residues. Overall, residues interactions play a major role in SARS-CoV-2's membrane protein agonist activity.

The top five hit compounds for the main protein, spike protein and membrane protein of SARS-CoV-2 were chosen for further validation through molecular dynamic simulation.

Molecular dynamics analysis

The MD simulation for the complexes was performed. The complex dynamics, evaluates protein flexibility and stability of the dynamic model. In addition, we found that all of the approaches were stable and that the simulations fell within an acceptable range.

Root mean square deviation

RMSD for back bone atomic value calculated to identify the structural changes and dynamic behavior of our protein complex. The RMSD plots of Main protein, spike protein and membrane protein with the screened top 5 compounds were obtained (Fig. 5A-C). In other criteria RMSD plots of Main protein with its top 5 compounds were displayed in figure.

In Main protein the top hits of 5 compounds chosen wereID-45273840, ID-44259144, ID-10121947, ID-5320835 and ID-5318767. The first RMSD of Main protein and 45273840 (Compound ID) ligand complexes reaches the value of 0.3 nm between 5 ns to 45 ns, followed by44259144 (Compound ID) ligand complexes reaches the value of 0.45 nm between 15 ns to 50 ns, 10121947 (Compound ID) ligand complexes reaches the value of 0.25 nm between 10 ns to 50 ns, 5320835 (Compound ID) ligand complexes reaches the value

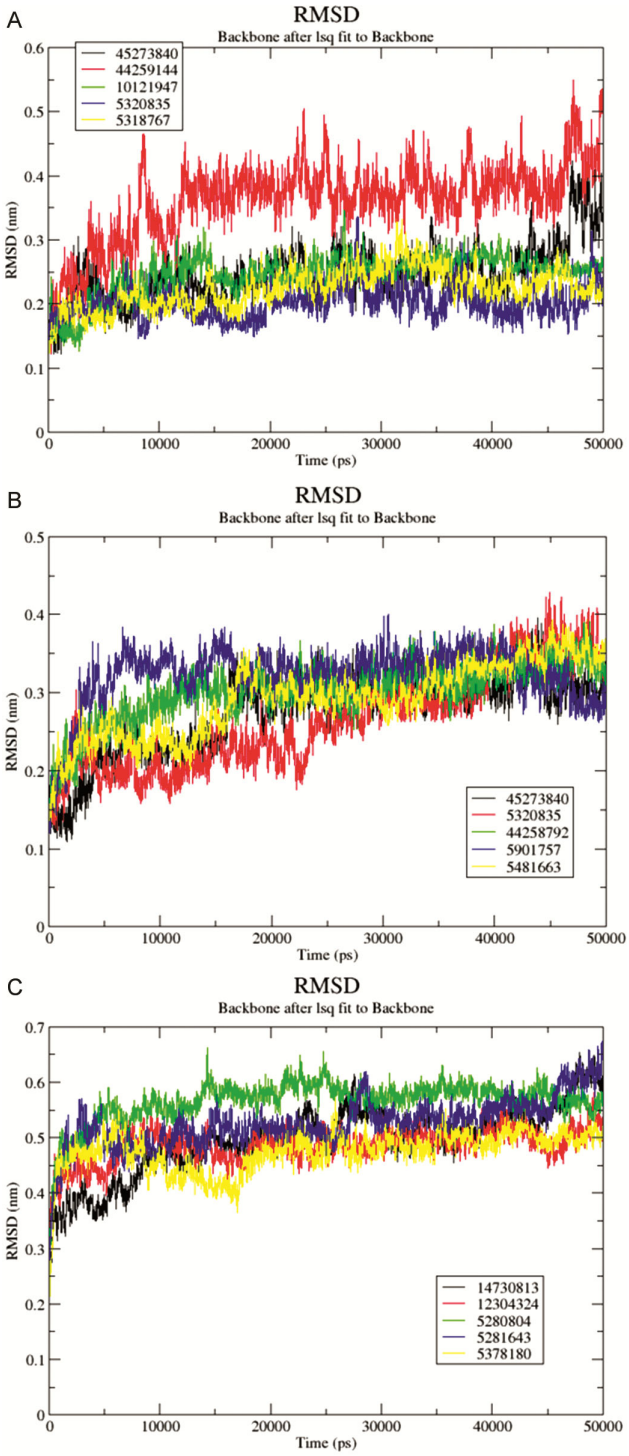

Fig. 5 — RMSD of SARS-CoV-2 (A) Main protein; (B) Spike protein; and (C) Membrane protein with *Moringa oleifera* leaves compound

of 0.25 nm between 5 ns to 50 ns and5318767 (Compound ID) ligand complexes reaches the value of 0.25 nm between 5 ns to 50 ns it reveals greater conformation stability of the protein–ligand complex (Fig. 5A).

In spike protein the top hits of 5 compounds chosen were ID-45273840, ID-5320835, ID-44258792, ID-5901757and ID-5481663. The first RMSD of spike protein and 45273840(Compound ID) ligand complexes reaches the value of 0.35 nm between 15 ns to 45 ns, followed by5320835(Compound ID) ligand complexes reaches the value of 0.3 nm between 20 ns to 40 ns, 44258792(Compound ID) ligand complexes reaches the value of 0.3 nm between 10 ns to 50 ns, 5901757(Compound ID) ligand complexes reaches the value of 0.35 nm between 10 ns to 50 ns and5481663(Compound ID) ligand complexes reaches the value of 0.35 nm between 18 ns to 50 ns it reveals greater conformation stability of the protein–ligand complexes (Fig. 5B).

In Membrane protein the top 5 hit compounds were chosen 14730813, 12304324, 5280804, 5281643, and 5378180. The first RMSD of membrane14730813 (Compound ID) ligand complexes reaches the value of 0.5 nm between 10 ns to 45 ns, followed by12304324 (Compound ID) ligand complexes reaches the value of 0.5 nm between 10 ns to 50 ns, 5280804 (Compound ID) ligand complexes reaches the value of 0.55 nm between 5 ns to 50 ns, 5281643 (Compound ID) ligand complexes reaches the value of 0.55 nm between 3 ns to 45 ns and 5378180 (Compound ID) ligand complexes reaches the value of 0.5 nm between 20 ns to 50 ns it reveals greater conformation stability of the protein–ligand complex (Fig. 5C).

Root-mean-square fluctuation

The root-mean-square fluctuation (RMSF) analysis describes the protein residue flexibility for 50 ns run. The RMSF value of docked complex has been calculated and plots in (Fig. 6A-C). The overall average RMSF values of In Main protein the top hits of 5 compounds chosen were ID-45273840, ID-44259144, ID-10121947, ID-5320835 and ID-5318767, In spike protein the top hits of 5 compounds chosen were ID-45273840, ID-5320835, ID-44258792, ID-5901757and ID-5481663, In Membrane protein the top 5 hit compounds were chosen 14730813, 12304324, 5280804, 5281643, and 5378180are calculated.

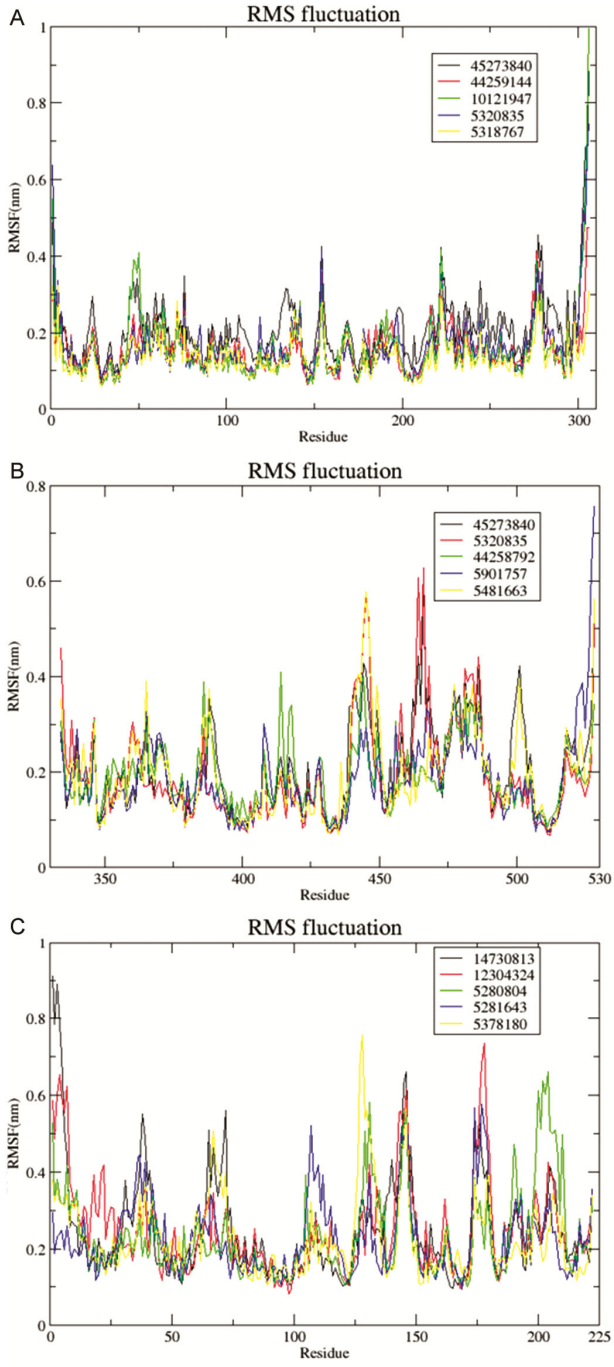

Fig. 6 — RMSF of SARS-CoV-2 (A) Main protein; (B) Spike protein; and (C) Membrane protein with *Moringa oleifera* leaves compound

Hydrogen bonding analysis

To determine the pace at which drugs binds to the active region/ site of SARS-CoV-2's structural proteins, studies examined the time dependence of the hydrogen bonds amongst drug-like molecules and

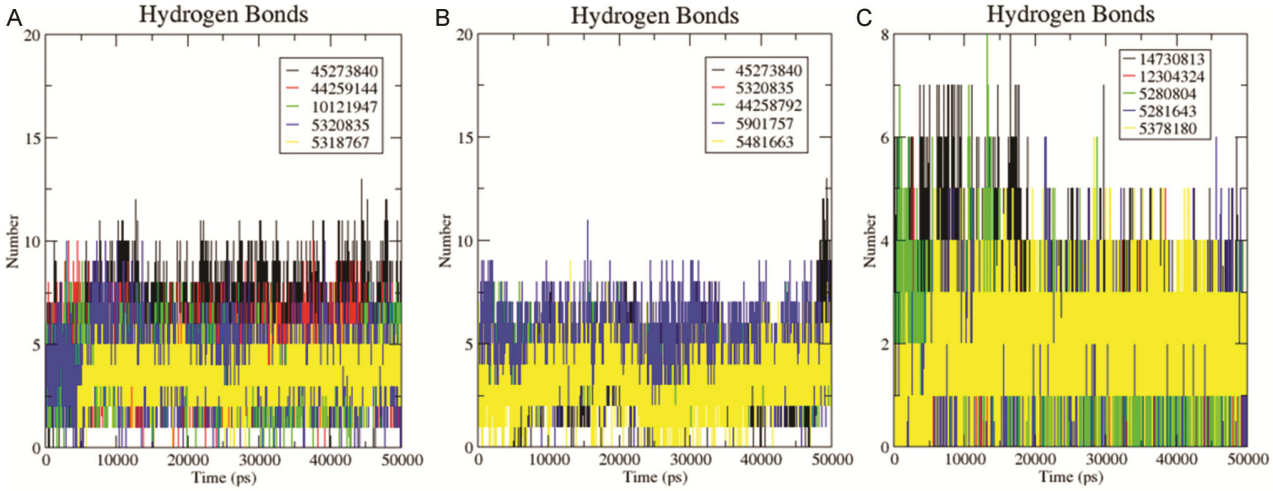

Fig. 7 — Hydrogen bond analysis of SARS-CoV-2 (A) Main protein; (B) Spike protein; and (C) Membrane protein with *Moringa oleifera* leaves compound

Table 5 — Density Functional Theory analysis for *Moringa oleifera* leaves compounds

S. No.	Compound Id	HOMO (eV)	LUMO (eV)	HLG (eV)	Solvation Energy (kcal/mol)
1	5280804	-0.213126	-0.055929	-0.157197	-36.43
2	5281643	-0.212246	-0.055690	-0.156556	-34.21
3	12304324	-0.214066	-0.056459	-0.157607	-31.17
4	5318767	-0.218749	-0.056785	-0.161964	-41.12
5	13915496	-0.216805	-0.057200	-0.159605	-36.22
6	5320835	-0.215902	-0.058247	-0.157655	-43.27
7	10121947	-0.211537	-0.063589	-0.147948	-33.42
8	6255	-0.243270	0.056442	-0.299712	-29.92
9	107876	-0.208284	-0.009306	-0.198978	-34.14
10	1794427	-0.193880	-0.062468	-0.131412	-78.93
11	10088114	-0.191816	-0.009378	-0.182438	-85.21
12	14730813	-0.196921	-0.055064	-0.141857	-90.71
13	71459647	-0.219730	-0.065758	-0.153972	-46.12
14	452738490	-0.248375	0.038744	-0.287119	-102.19
15	44259144	-0.210988	-0.057126	-0.153862	-65.73
16	44258792	-0.216835	-0.059944	-0.156891	-73.14
17	10929258	-0.214540	-0.066797	-0.147743	-109.76
18	5901757	-0.220624	-0.064833	-0.155791	-60.36
19	5481663	-0.216258	-0.062458	-0.1538	-57.40
20	5280805	-0.214897	-0.061342	-0.153555	-67.97
21	5378180	-0.220051	-0.060786	-0.159265	-46.73
22	9851181	-0.222731	-0.066038	-0.156693	-54.32
23	6474640	-0.214324	-0.067999	-0.146325	-109.00

receptors over the period of simulations. The finding indicated a connection between the biological effects of its most effective inhibitory drugs and the recently identified intermolecular bonding of hydrogen. The *Moringa oleifera* leaves compound has a sustained hydrogen bonds interacts throughout the simulation, which suggested that it might be favorable for complexes (Fig. 7A-C).

DFT Calculations

Jaguar module of Schrodinger software was performed to calculate the DFT for the top hits. The HOMO and LUMO values calculation for *Moringa oleifera* leaves compounds and the values ranges from -0.191816 to -0.248375, and -0.009306 to 0.056442, which was shown in (Table 5 and Fig. 8).

The ligands DFT results prove that they have a higher electron donor and acceptor activity, and the

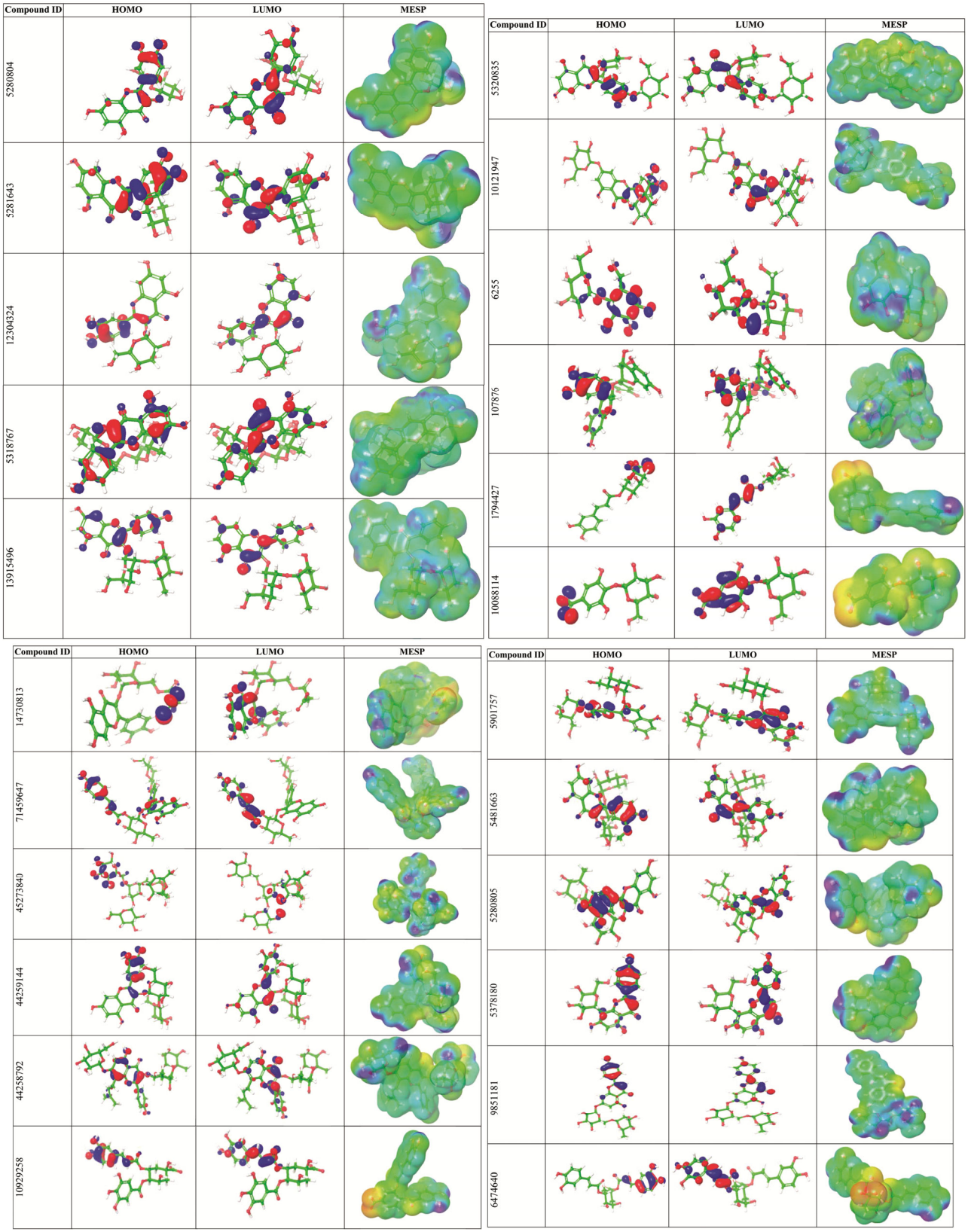

Fig. 8 — DFT calculations of *Moringa oleifera* leaves compound for SARS-CoV-2 structural proteins

Table 6 — ADME analysis for *Moringa oleifera* leaves compounds

Compound ID	QPlogPo/w	QPlogBB	QPPMDCK	QPPCaco	Rule Of Five	Human Oral Absorption	Percent of Human Oral Absorption
6255	-3.661	-2.66	5.485	15.528	2	1	0.911
107876	0.076	-4.956	0.127	0.476	3	1	0
1794427	-0.25	-3.317	0.666	1.768	1	1	16.949
5280804	-1.463	-3.727	0.717	2.363	2	1	0
5280805	-2.695	-5.29	0.096	0.368	3	1	0
5281643	-1.428	-3.69	0.81	2.646	2	1	0.229
5318767	-2.08	-3.822	0.528	1.782	3	1	0
5320835	-3.521	-5.879	0.042	0.17	3	1	0
5378180	-0.843	-2.948	1.989	6.074	1	2	23.073
5481663	-1.867	-3.75	0.922	2.984	3	1	0
5901757	-2.552	-4.376	0.597	1.994	3	1	0
6474640	0.73	-4.791	0.146	0.433	3	1	0
9851181	-1.371	-4.119	1.246	3.942	3	1	0
10088114	-1.981	-3.195	0.424	1.164	1	1	3.567
10121947	-3.465	-5.75	0.067	0.263	3	1	0
10929258	-0.282	-5.215	0.037	0.123	3	1	0
12304324	-1.416	-3.355	1.319	4.155	2	1	3.808
13915496	-1.73	-3.485	1.937	5.927	3	1	0
14730813	-0.496	-4.021	0.136	0.406	3	1	0
44258792	-1.648	-5.944	0.198	0.717	3	1	0
44259144	-3.234	-4.97	0.145	0.539	3	1	0
45273840	-9.987	-8.027	0.004	0.018	3	1	0
71459647	-1.222	-7.307	0.037	0.151	3	1	0

data were trustworthy for docking. The top fifteen compounds, MESP's stereo electrical property, as well as additional properties including solvation energy, HOMO, and LUMO, was shows in (Fig. 8). The highest hit compound solvation energies of *Moringa oleifera* range from -29.92 to -109.76 kcal/mol (Table 5). The compounds exhibited more soluble in water as evidenced by the solvation energy values, which were higher negative value range. The results allow us to calculate the ligands solvation energies, which is essential for determining the compound's water solubility. Overall, the DFT was used to establish the replacement effects in protein-ligand interactions and compound molecular stability.

ADME prediction

The ADME identifies SARS-CoV-2's potential antagonist compounds using QikProp module. The list of descriptors with drug-likeness results including rule of five was tabulated (Table 6). The ADME prediction using *in silico* is essential for predicting the molecules biological effect before proceeding with experimental testing. The Qplogpo/w of partial coefficient determines the ratio concentration ranges from -9.987 to 0.735. The QPPCaco value determines drug metabolism in human body conditions from 0.018 to 15.528. The drug HOA was estimated ranging from 1 to 2. The observations of ADME results for all the screened compounds have acceptable range and it attains the drug-likeness property (Table 6). Further these drugs are found within the range of acceptance and had a potent drug-likeness property for humans.

Toxicity prediction

The ProTox-II is a online server used for predicting the toxicity profile for the selected compounds. The results assisted to define the organ toxicity and toxicity end points criteria. All compounds obtained are classified from class III to class V, acceptable in range and may need to be modified if adverse reactions are observed (Table 7). The LD50 value for the compounds ranges from 51 to 5000 mg/kg. The predictions have a range of probability from 0.52 to 0.99. The Fifteen reported compounds of showed better toxicity profiles. Overall, the obtained hits showed the normalized toxicity level. The validation can further tested in *in vitro* and *in vivo* analysis for confirming permissible toxicity profile.

Table 7 — Toxicity analysis of *Moringa oleifera* leaves compounds

S. No.	Compound Id	Predicted LD50 mg/kg	Predicted toxicity class	Hepatotoxicity	Carcinogenicity	Immunotoxicity	Mutagenicity	Cytotoxicity
1	45273840	51	III	Inactive (0.91)	Inactive (0.93)	Inactive (0.96)	Inactive (0.88)	Inactive (0.79)
2	44259144	5000	V	Inactive (0.83)	Inactive (0.85)	Active (0.94)	Inactive (0.74)	Inactive (0.67)
3	10121947	5000	V	Inactive (0.83)	Inactive (0.85)	Active (0.71)	Inactive (0.74)	Inactive (0.67)
4	5320835	5000	V	Inactive (0.83)	Inactive (0.85)	Active (0.85)	Inactive (0.74)	Inactive (0.67)
5	5318767	5000	V	Inactive (0.80)	Inactive (0.91)	Active (0.95)	Inactive (0.88)	Inactive (0.64)
6	5280805	5000	V	Inactive (0.80)	Inactive (0.91)	Active (0.98)	Inactive (0.88)	Inactive (0.64)
7	12304324	5000	V	Inactive (0.82)	Inactive (0.85)	Active (0.66)	Inactive (0.76)	Inactive (0.69)
8	71459647	5000	V	Inactive (0.80)	Inactive (0.85)	Active (0.99)	Active (0.53)	Inactive (0.71)
9	44258792	5000	V	Inactive (0.73)	Inactive (0.82)	Active (0.99)	Inactive (0.68)	Inactive (0.66)
10	5901757	5000	V	Inactive (0.85)	Inactive (0.9)	Active (0.93)	Inactive (0.69)	Inactive (0.55)
11	5481663	5000	V	Inactive (0.81)	Inactive (0.93)	Active (0.99)	Inactive (0.90)	Inactive (0.52)
12	6255	51	III	Inactive (0.91)	Inactive (0.93)	Inactive (0.97)	Inactive (0.88)	Inactive (0.79)
13	13915496	5000	V	Inactive (0.81)	Inactive (0.90)	Active (0.98)	Inactive (0.73)	Inactive (0.66)
14	14730813	5000	V	Inactive (0.84)	Inactive (0.82)	Inactive (0.57)	Inactive (0.58)	Inactive (0.67)
15	107876	2170	V	Inactive (0.76)	Inactive (0.60)	Inactive (0.70)	Inactive (0.73)	Inactive (0.74)
16	10088114	3750	V	Inactive (0.87)	Inactive (0.76)	Inactive (0.98)	Inactive (0.77)	Inactive (0.87)
17	5280804	5000	V	Inactive (0.82)	Inactive (0.85)	Active (0.66)	Inactive (0.76)	Inactive (0.69)
18	5281643	5000	V	Inactive (0.82)	Inactive (0.85)	Active (0.66)	Inactive (0.76)	Inactive (0.69)
19	5378180	832	IV	Inactive (0.81)	Inactive (0.72)	Inactive (0.82)	Active (0.52)	Inactive (0.87)
20	1794427	5000	V	Inactive (0.72)	Inactive (0.68)	Active (0.99)	Inactive (0.93)	Inactive (0.80)
21	9851181	5000	V	Inactive (0.81)	Inactive (0.91)	Active (0.76)	Inactive (0.68)	Inactive (0.65)
22	10929258	3800	V	Inactive (0.71)	Inactive (0.67)	Active (0.99)	Inactive (0.86)	Inactive (0.83)
23	6474640	5000	V	Inactive (0.71)	Inactive (0.65)	Active (0.98)	Inactive (0.85)	Inactive (0.84)

Conclusion

The processing of moringa leaves at 60°C for 2 h increased the quantity of phenols and flavonoid components in tea, which promote and regulates as an immune booster for the human health. According to the study, moringa tea or soup is a high phenolic and flavonoids-rich beverage with antioxidant property. Value added products like tea prepared from moringa can be affordable by all socio-economic people and improve their health benefits. The moringa leaves were rich in nutritional content and function as an immune booster against SARS-CoV-2. This article's overview opens the path for the nutrigenomics approach and targeted structural proteins (Main protein, Spike glycoprotein and Membrane protein) research using the *in-silico* technique and screened moringa leaves compounds. The virtual screening was employed for the SARS-CoV-2 structural proteins. Overall, the screened compounds from the Moringa leaves were targeted for SARS-CoV-2 structural proteins. Among the compounds from *Moringa oleifera* the compounds D-Glucopyranosyl) -(alpha-1,6)-(D-glucopyranosyl)-(alpha-1,6)-(3-O-[D-glucopyranosyl)-(alpha-1,3)]-D-glucopyranosyl)-(alpha-1,6)-alpha/beta-D-glucopyranoside has better potential inhibitory profile because inhibits or binds to two structural proteins (main protein and Spike protein) of SARS-CoV-2. As a result, this obtained compounds from the Moringa leaves show a potent antagonist activity against SARS-CoV-2's structural proteins. Along with specific medicine the agonist/ vaccines of SARS-CoV-2, this whole extract tea/ soup of moringa leaves helps patients to overcome out of clinical pathogenesis; because several compounds present in moringa leaves binds to major structural protein of SARS-CoV-2. So that it could be a good alternative supplementary food product to overcome with the disease pathogenesis. Thus, the *in silico* approach paves the way for understanding the action mechanism of moringa leaves compounds against SARS-CoV-2's structural proteins.

Acknowledgement

The authors PR, PP, and AJ thank the SEED Division under the Department of Science and Technology, New Delhi, India for the financial support (SEED/WS/018/2011) provided to carry out this research work. The authors MJ, SS and KM are thankfully acknowledging the MHRD-RUSA 2.0 - F.24/51/2014-U, Policy (TNMulti-Gen), Dept. of Education, and DBT-BIC/No.BT/PR40154/BTIS/ 137/34/2021, Govt. of India for the financial supports

and infrastructure facilities and Authors MP and AGAS are thankful to Institute of Research and Consulting Studies (grant number: 3-N-20/21), King Khalid University.

Conflict of interest

All authors declare no conflict of interest.

References

1 Islam Z, Islam SM, Hossen F, Mahtab-ul-Islam K, Hasan MR & Karim R, *Moringa oleifera* is a prominent source of nutrients with potential health benefits. *Int J Food Sci*, 6627265 (2021).

2 Patil SV, Mohite BV, Marathe KR, Salunkhe NS, Marathe V & Patil VS, Moringa Tree, Gift of Nature: a Review on Nutritional and Industrial Potential. *Curr Pharmacol Rep*, 8 (2022) 262.

3 Agrawal ND, Nirala SK, Bhadauria M, Srivastava S & Shukla S, Protective potential of *Moringa oleifera* Lam. along with curcumin and piperine against beryllium-induced alterations in hepatorenal biochemistry and ultramorphology in rats. *Indian J Biochem Biophys,* 56 (2019) 70.

4 Rajkumar R, Ilang B, Vinothkumar K, Savidha R, Senthilkumar S, Ezhilarasan D & Sukumar E, *Moringa oleifera* seeds attenuate benzene-induced alterations in lipid peroxidation and antioxidant enzymes in liver and kidney tissues of Wistar rats. *Indian J Biochem Biophys*, 60 (2023) 26.

5 Behl T, Kumar K, Brisc C, Rus M, Nistor-Cseppento DC, Bustea C, Aron RAC, Pantis C, Zengin G, Sehgal A & Kaur R, Exploring the multifocal role of phytochemicals as immunomodulators. *Biomed Pharmacother*, 133 (2021) 110959.

6 Masih LP, Singh SU, Elamathi S, Anandhi P & Abraham TH, Moringa: A multipurpose potential crop-A review. *Proc Indian National Sci Acad*, 85 (2019) 589.

7 Bindu H, Bhuvaneshwari G, Jagadeesh SL, Ganiger VM, Rudresh DL & Kumar B, Evaluation of physical and functional properties of weaning food blended with banana, sweet potato and drumstick leaves powder. *J Pharmacogn Phytochem*, 8 (2019) 1568.

8 Giuberti G, Rocchetti G, Montesano D & Lucini L, The potential of *Moringa oleifera* in food formulation: A promising source of functional compounds with health-promoting properties. *Curr Opin Food Sci*, 42 (2021) 257.

9 Deepa J & Revanna ML, Nutrient Composition of Drumstick Leaves (*Moringa oleifera*) with Different Drying Methods. *Mysore Journal of Agricultural Sciences* (*MJAS*), 53 (2019) 94.

10 Olusanya RN, Kolanisi U, Van Onselen A, Ngobese NZ & Siwela M, Nutritional composition and consumer acceptability of *Moringa oleifera* leaf powder (MOLP)-supplemented mahewu. *South Afr J Bot*, 129 (2020) 175.

11 Olumide M.D, Ajayi OA & Akinboye OE, Comparative study of proximate, mineral and phytochemical analysis of the leaves of *Ocimum gratissimum*, *Vernonia amygdalina* and *Moringa oleifera*. *J Med Plants Res*, 13 (2019) 351.

12 Kashyap P, Kumar S, Riar CS, Jindal N, Baniwal P, Guiné RP, Correia PM, Mehra R & Kumar H, Recent advances in Drumstick (*Moringa oleifera*) leaves bioactive compounds: Composition, health benefits, bioaccessibility, and dietary applications. *Antioxidants*, 11 (2022) 402.

13 Nuertey BD, Addai J, Kyei-Bafour P, Bimpong KA, Adongo V, Boateng L, Mumuni K, Dam KM, Udofia EA, Seneadza NA & Calys-Tagoe BN, Home-Based Remedies to Prevent COVID-19-Associated Risk of Infection, Admission, Severe Disease, and Death: A Nested Case-Control Study. *eCAM*, (2022).

14 Siddiqui S, Upadhyay S, Ahmad R, Barkat MA, Jamal A, Alothaim AS, Hassan MZ, Rahman MA, Arshad M, Ahamad T & Khan MF, Interaction of bioactive compounds of *Moringa oleifera* leaves with SARS-CoV-2 proteins to combat COVID-19 pathogenesis: A phytochemical and *in silico* analysis. *Appl Biochem Biotechnol*, 194 (2022) 5918.

15 Jayaraj JM, Jothimani M, Palanisamy CP, Pentikäinen OT, Pannipara M, Al-Sehemi AG, Muthusamy K & Gopinath K, Computational study on the inhibitory effect of natural compounds against the SARS-CoV-2 proteins. *Bioinorg Chem Appl*, (2022).

16 Preethi R, Deotale SM, Moses JA & Anandharamakrishnan C, Conductive hydro drying of beetroot (*Betavulgaris* L) pulp: Insights for natural food colorant applications. *J Food Process Eng*, 43 (2020) e13557.

17 Zohmachhuana A, Vabeiryureilai M, Meitei Thangjam N, Lalrinzuali K, Senthil Kumar N & Kumar A, Antioxidant efficacy and cytotoxicity of ethanol extract of *Clerodendrum infortunatum* against different cell lines. *Indian J Biochem Biophys*, 58 (2021) 6.

18 Nagaraj A, Kalagatur NK, Kadirvelu K, Shankar S, Mangamuri UK, Sudhakar P & Samiappan S, Biomimetic of hydroxyapatite with Tridax procumbens leaf extract and investigation of antibiofilm potential in *Staphylococcus aureus* and *Escherichia coli*. *Indian J Biochem Biophys*, 59 (2022) 755.

19 Yang J, Yan R, Roy A, Xu D, Poisson J & Zhang Y, The I-TASSER Suite: protein structure and function prediction. *Nat Methods*, 12 (2015) 7.

20 Loganathan L, Natarajan K & Muthusamy K, Computational study on cross-talking cancer signalling mechanism of ring finger protein 146, AXIN and Tankyrase protein complex. *J Biomol Struct Dyn*, 38 (2020) 5173.

21 Kirubakaran P, Kothandan G, Cho SJ & Muthusamy K, Molecular insights on TNKS1/TNKS2 and inhibitor-IWR1 interactions. *Mol Biosyst*, 10 (2014) 281.

22 Loganathan L, Muthusamy K, Jayaraj JM, Kajamaideen A & Balthasar JJ, *In silico* insights on tankyrase protein: A potential target for colorectal cancer. *J Biomol Struct Dyn*, (2018).

23 Friesner RA, Murphy RB, Repasky MP, Frye LL, Greenwood JR, Halgren TA, Sanschagrin PC & Mainz DT, Extra precision glide: Docking and scoring incorporating a model of hydrophobic enclosure for protein− ligand complexes. *J Med Chem*, 49 (2006) 6177.

24 Jenny J & Kumar PB, Dihydroxy berberine from *Tinospora cordifolia*: *in silico* evidences for the mechanism of anti-inflammatory action through dual inhibition of Lipoxygenase and Cyclooxygenase. *Indian J Biochem Biophys*, 58 (2021) 244.

25 Saila MH & Thakur S, Molecular docking analysis of phytoconstituents of *Illicium verum* fruit against Caspase 3, MMP-9 and TNF-α. *Indian J Biochem Biophys,* 58 (2021) 510.

26 Bochevarov AD, Harder E, Hughes TF, Greenwood JR, Braden DA, Philipp DM, Rinaldo D, Halls MD, Zhang J & Friesner RA, Jaguar: A high-performance quantum chemistry software program with strengths in life and materials sciences. *Int J Quantum Chem*, 113 (2013) 2110.

27 Çakmak Ş & Erdoğan T, Some bis (3-(4-nitrophenyl) acrylamide derivatives: Synthesis, characterization, DFT, antioxidant, antimicrobial properties, molecular docking and molecular dynamics simulation studies. *Indian J Biochem Biophys,* 60 (2023) 209.

28 He L, Liu J, Zhao HL, Zhang LC, Yu RL & Kang CM, De novo design of dual-target JAK2, SMO inhibitors based on deep reinforcement learning, molecular docking and molecular dynamics simulations. *Biochem Biophys Res Commun*, 638 (2023) 23.

29 Wacha A, Varga Z & Beke-Somfai T, Comparative Study of Molecular Mechanics Force Fields for β-Peptidic Foldamers: Folding and Self-Association. *J Chem Inf Model*, (2023).

30 Ashiru MA, Ogunyemi SO, Temionu OR, Ajibare AC, Cicero-Mfon NC, Ihekuna OA, Jagun MO, Abdulmumin L, Adisa QK, Asibor YE & Okorie CJ, Identification of EGFR inhibitors as potential agents for cancer therapy: pharmacophore-based modeling, molecular docking, and molecular dynamics investigations. *J Mol Model*, 29 (2023) 128.

31 Madhana Priya N, Archana Pai P, Kumar TD, Gnanasambandan R & Magesh R, Elucidating the functional impact of G137V and G144R variants in Maroteaux Lamy's Syndrome by Molecular Dynamics Simulation. *Mol Divers*, (2023) 1.

32 Saffari-Chaleshtori J, Shafiee SM & Heidarian E, The effect of bilirubin on Bad, Bak, and Bim pro-apoptotic factors: A molecular dynamic simulation study. *Indian J Biochem Biophys*, 58 (2021) 236.

33 Muniyasamy H, Aravind MK, Malaisamy AK, Balasubramaniem AK, Sepperumal M & Ayyanar S, Pharmacophore-based Synthesis of Pyrazole Analogues as Artificial Antibiotics Targeting Salmonella Typhi. *J Mol Struct*, (2023) 136801.

34 Toppo AL, Yadav M, Dhagat S, Ayothiraman S & Eswari JS, Molecular docking and ADMET analysis of synthetic statins for HMG-CoA reductase inhibition activity. *Indian J Biochem Biophys*, 58 (2021) 127.

35 Katiyar K, Kumar Srivastava R, Nath R & Singh G, Cryptosporidiosis, a public health challenge: A combined 3D shape-based virtual screening, docking study, and molecular dynamics simulation approach to identify inhibitors with novel scaffolds for the treatment of cryptosporidiosis. *Indian J Biochem Biophys*, 59 (2022) 296.

36 Banerjee P, Eckert AO, Schrey AK & Preissner R, ProTox-II: a web server for the prediction of toxicity of chemicals. *Nucleic Acids Res*, 46 (2018) W257.

37 Soares S, Brandão E, Guerreiro C, Soares S, Mateus N & de Freitas V, Tannins in Food: Insights into the Molecular Perception of Astringency and Bitter Taste. *Molecules*, 25 (2020) 2590.

38 Shi Q, Li X, Du J, Liu Y, Shen B & Li X, Association of Bitter Metabolites and Flavonoid Synthesis Pathway in Jujube Fruit. *Front Nutr*, 9 (2022) 901756.

39 Saini RK, Sivanesan I & Keum YS, Phytochemicals of Moringa oleifera: a review of their nutritional, therapeutic and industrial significance. *Biotech*, 6 (2016) 1.

40 Mansour HM, Hamideldin N, Hassan YE & Saleh OM, Influence of gamma irradiation pre-sowing treatments on the seeds yield of *Moringa oleifera*. *Radiat Environ Biophys*, (2023) 30.

41 Daniel A, Engeda D & Chetan C, Effect of thermal treatment on phenolic content, antioxidant, and-amylase inhibition activities of *Moringa stenopetala* leaves. *Afr J Food Sci*, 9 (2015) 487.

42 Pham HN, Nguyen VT, Vuong QV, Bowyer MC & Scarlett CJ, Effect of extraction solvents and drying methods on the physicochemical and antioxidant properties of *Helicteres hirsuta* Lour. leaves. *Technologies*, 3 (2015) 285.

43 Ueda Y, Matsuda Y, Murata T, Hoshi Y, Kabata K, Ono M, Kinoshita H, Igoshi K & Yasuda S. Increased phenolic content and antioxidant capacity of the heated leaves of yacon (*Smallanthus sonchifolius*). *Biosci Biotech Biochem,* 83 (2019) 2288.

44 Ghafoor K, Ahmed IAM, Doğu S, Uslu N, Fadimu GJ, Al Juhaimi F, Babiker EE & Özcan MM, The effect of heating temperature on total phenolic content, antioxidant activity, and phenolic compounds of plum and mahaleb fruits. *Int J Food Eng,* 15 (2019) 20170302.